Displacement sensor based on polarization mixture of orthogonal polarized He-Ne laser at 1.15 μm

Zhengqi Zhao (赵正启), Shulian Zhang (张书练)*, Peng Zhang (张 鹏), Zhaoli Zeng (曾召利), Yidong Tan (谈宜东), and Yan Li (李 岩)

State Key Laboratory of Precision Measurement Technology and Instruments, Department of Precision Instruments and Mechanology, Tsinghua University, Beijing 100084, China

**Corresponding author: zsl-dpi@mail.tsinghua.edu.cn*

Received July 15, 2011; accepted September 23, 2011; posted online November 18, 2011

Displacement sensor based on the polarization mixture and the cavity tuning of the orthogonal polarized He-Ne laser 1.15 μm is presented. The power tuning curves of He-Ne laser are irregular, and it is difficult to measure the change in cavity length. The distortion of the curves is caused by the higher relative excitation compared with the He-Ne laser at 633 nm. In view of its potential for the wider displacement measuring range, a new method of displacement sensing is developed. Experiments show that displacement measuring stability based on the method of the polarization mixture is better than that of the power tuning curves. The displacement sensor achieves the measuring range of 100 mm, resolution of 144 nm, and linearity of 7×10^{-6}.

OCIS codes: 280.3420, 140.1340, 260.5430
doi: 10.3788/COL201210.032801.

The applications of laser technology are widely used in metrology because of the traceability to the wavelength[1,2]. Many characteristics and applications of laser, such as spectrum, wavelength, beat frequency, intensity, laser line, and fringes, are used in different measurement areas[3−7]. In most of these applications, laser is regarded as a source of light with excellent performance, including having high intensity, stability, and directionality. Another important factor in displacement measurement is the stability of frequency because frequency is directly related to result of measurement. Hence, the frequency stabilization system is necessary in a high-precision measuring system, which results in a complex structure.

Intracavity tuning displacement sensing is the application of the intracavity laser method in the field of displacement measurement. Du *et al.*[8] utilized a dual-frequency He-Ne laser at 633 nm as a displacement sensor, with the measuring range being 12 mm. It has the merits of linearity, self-calibration, and traceability to the wavelength. The simple structure also has stability. The frequency stabilization system is not necessary and the cost is much lower. However, the measuring range can hardly be increased because the measuring method requires the operation of a single longitudinal mode. During the process of measurement, the vibration of the cavity mirror may lead to the detuning of the laser cavity, and the output light disappears when the loss surpasses the gain. Research shows that He-Ne laser at 1.15 μm is more promising for the intracavity laser method, because the active medium gain of the laser is more than that of He-Ne laser at 633 nm. Therefore, in theory, the adoption of He-Ne laser at 1.15 μm can enlarge the measurement range.

The active medium of He-Ne laser is mainly Doppler broadened. The laser line function $g_{\rm D}(v, v_0)$ is in the form of a Gaussian shape. When v equals v_0, $g_{\rm D}(v, v_0)$ reaches the maximum[9]:

$$g_{\rm Dmax} = \lambda\Big(\frac{m}{2\pi k_{\rm b}T}\Big), \tag{1}$$

where v_0 is the central frequency, λ is the wavelength of the laser, m is the atomic mass, $k_{\rm b}$ is the Boltzmann constant, and T is the temperature. The corresponding gain factor G can be expressed as

$$G = \Delta n \frac{v^2 A_{21}}{8\pi c^2}\left(\frac{m}{2\pi k_{\rm b}T}\right)^{1/2}\lambda^3, \tag{2}$$

where Δn is the inverted population density, v is the velocity of atoms, and A_{21} is the spontaneous emission rate. Equation (2) shows that G is proportional to λ^3. This means that the gain of the laser will be higher for a longer wavelength with the same active medium and conditions. Higher gain promises a wider displacement measurement range and stability, thus He-Ne laser at 1.15 μm is more suitable to be a displacement sensor.

After inserting a birefringence element (such as a quartz plate, a stress-birefringence glass, etc.) into the laser cavity, one geometric cavity length becomes a cavity with two physical lengths. One laser beam then splits into two orthogonal linear polarized beams with a certain frequency difference[10,11]. They can be called o-light and e-light, respectively, according to crystal optics. The cavity tuning characteristics of the orthogonally polarized dual-frequency He-Ne laser at 1.15 μm have been discussed in detail[12].

The schematic structure of the experimental setup is shown in Fig. 1. A half-intracavity cavity laser is composed of a concave output mirror M, a cat's eye reflector (CER), and a He-Ne laser discharge tube T. W refers to the window plate with an anti-reflection coating on both surfaces; Q is a quartz plate, which is obliquely placed to keep a certain angle between the crystal axis and the laser axis, and the frequency difference is adjusted by the

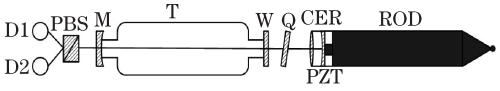

Fig. 1. Schematic structure of the experimental setup.

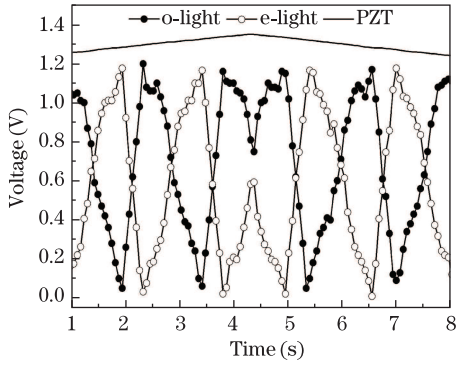

Fig. 2. Experimental results of the power tuning curves.

angle; PZT is a piezoelectric ceramic, and its elongation is linear with the supply voltage; ROD is the rod that moves in axial direction in a sleeve. CER, PZT, and ROD are mounted together. PBS is a Wollaston prism used to separate two orthogonal polarized linear beams. D1 and D2 are two photoelectrical detectors. Two beams are the output from M, separated by PBS, and then projected on D1 and D2.

CER is composed of a convex lens and a concave mirror. There are anti-reflection coatings on both surfaces of the convex lens and a high reflective coating (>99.9%) on the left-hand side of the concave mirror, as shown in Fig. 1. The focal length of the convex lens, the radius of the curvature of the concave mirror, and the distance between them are equal. A normal incident paraxial beam will be reflected back by CER along the entrance way. Even for the obliquely incident paraxial beam (the tilt angle is small enough), CER can still provide high parallelism for the incident and reflected beam. This is the reason why CER, acting as a resonator mirror, can improve laser stability. This is impossible for any traditional laser resonator mirror. If there is slight vibration in the process of displacement measurement, the application of CER can reduce the destructive influence[13].

All parameters of the discharge tube T are selected through a series of experiments. The length of the capillary is 90 mm, and the diameter is 1.5 mm. The transmittance of M is 2.5%, and the radius of the curvature is 1 m. The pressure is 500 Pa, and He^3:Ne^{20}:Ne^{22} equals 9:0.5:0.5. The discharge current is 3 mA. All the coatings above are for the wavelength of 1.15 μm. PZT is driven by the triangular supply voltage, hence the cavity length changes forward and backward in the short scale. The corresponding power tuning curves are shown in Fig. 2.

The result shows that the power tuning curves deviate from the Gauss shape. Numerical calculation indicates that the distortion of power tuning curves is a combined action of the self-saturation and cross-saturation effects[12]. The power tuning curves are irregular and not fit for the direction judgment of the displacement. Although the magnitude relationship of the adjacent voltages where o-light equals e-light differ, the difference is too small to be distinguished exactly.

In view of its potential for the wider displacement measuring range, we look for a new method of displacement sensing. By rotating the Wollaston prism at a certain angle, o-light and e-light are mixed unequally, resulting in the creation of two new signals to reflect the judgment information of the displacement. Through this process, the total signal magnitude is compressed and the magnitude difference between the adjacent voltages where o-light equals e-light is maintained. The signals created by the polarization mixture are shown in Fig. 3.

In Fig. 3, the "x-light" and "y-light" mean that the main parts of the signal are separately composed of o-light and e-light. According to polarization optics, the intensities of x-light and y-light — I_x and I_y, respectively — can be expressed as

$$I_{x/y} = k \times I_{\mathrm{o/e}} + (1-k) \times I_{\mathrm{e/o}}, \tag{3}$$

where k is the proportion of I_{o} in the direction of x-light and $(1-k)$ is the proportion of I_{o} in the direction of y-light; they are determined by the rotation of the Wollaston prism. The sequence of the two signals is opposite when PZT moves forward or backward. This provides us with a method for displacement measurement, especially direction judgment. The signal-processing circuit is designed as:

(a) A high-pass filter is designed so that the mean value of the signal would be zero. The CER is modulated by PZT with high frequency.

(b) Generate a floating threshold for the purpose of

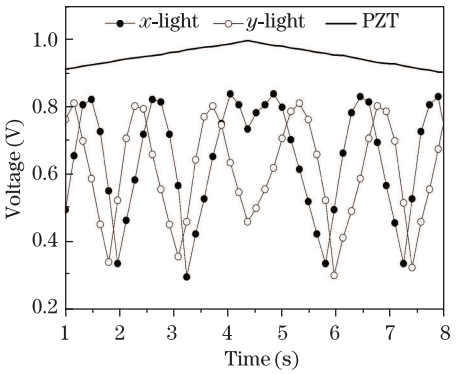

Fig. 3. Signals created by the polarization mixture.

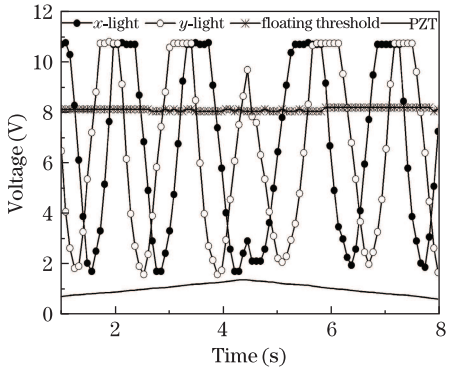

Fig. 4. Signals after the amplifier and the floating threshold.

subdivision. The floating threshold is calculated as the mean value of the adjacent high and low voltages where x-light equals y-light. It is also shown in Fig. 4.

(c) Generate a counting pulse where the voltage of the signal equals the floating threshold. The direction represented by the pulse is judged by the resulting sequence of x-light and y-light. As seen in Fig. 4, when the voltage of PZT increases, which means that the cavity length is shortened, y-light appears earlier than x-light; when the voltage of PZT decreases, x-light appears earlier than y-light. This phenomenon is used for direction judgment with the help of numerical logical chips. A numeric logical formula is established to count the pulses and judge the direction synchronously.

Within each longitudinal mode interval, four pulses exist. Each pulse represents $\lambda/8$; in this case, it is 144 nm. The equality of the interval of adjacent pulses is determined by the beat frequency, which is controlled by the rotation of the quartz crystal. The shape of the signals is well maintained during the ROD's moving range of 100 mm.

The accuracy of the system is tested by comparing it with a dual-frequency laser interferometer (Agilent 5529A). The linear motion of the translation stages for 100 mm is measured. The cube corner of the dual-frequency laser interferometer is fixed on the platform of the translation stages. The ROD of the displacement sensor is attached to the back of the cube corner. The axes of the displacement sensor, the dual-frequency laser, and the translation stages are placed on the same line. Therefore, the displacement of the translation stages is shown synchronously by the displacement sensor and the dual-frequency laser, and their measuring results are stored. Figure 5 shows the comparison of the results and the residual error.

The displacement sensor offers excellent repeatability. The results of multiple measurement of the same displacement are identical. The linearity in the range of 100 mm is 7×10^{-6} and the total uncertainty is estimated to be 459 nm. The details are as follows:

(a) The limitation of resolution causes the uncertainty of 144 nm.

(b) The inequality of the intervals of count pulse causes the uncertainty of about 30 nm. This is experimentally tested from the analysis of the waveform diagram.

(c) The change in the temperature of the laser cavity causes the uncertainty of about 432 nm. This is experimentally tested from the zero drift of the sensor, which is 432 nm per hour after the thermal balance. This is the combined action of the environment, while the main factor is the temperature.

(d) The gap between the rod and the sleeve causes the uncertainty of 50 nm. This is determined by the machining accuracy.

(e) The measurement of the wavelength causes the uncertainty of 0.01 nm.

When the cavity length changes in the measuring range, the change in magnitude of the signals created by the polarization mixture is much less than that of the power tuning curves because of the polarization mixture and the high-pass filter. As shown in Fig. 6, the magnitude of the power tuning curves changes by 300% compared with the lowest magnitude, while the magnitude of the signals created by the polarization mixture changes by 20%. The method of the polarization mixture ensures that the displacement sensor still works well when the cavity mirror is not well aligned. Thus, the displacement measuring stability based on the method of the polarization mixture is better than that of the power tuning curves.

In conclusion, a displacement sensor based on the polarization mixture and the cavity tuning of the orthogonal polarized He-Ne laser at 1.15 μm is demonstrated. By mixing the orthogonal polarized laser beams unequally, two signals are created to reflect the direction information of the displacement. A corresponding signal-processing circuit is designed with the function of a high-pass filter and the floating threshold generation. Subdivision pulses for the displacement counting and direction judgment are generated. Comparing the results with a dual-frequency

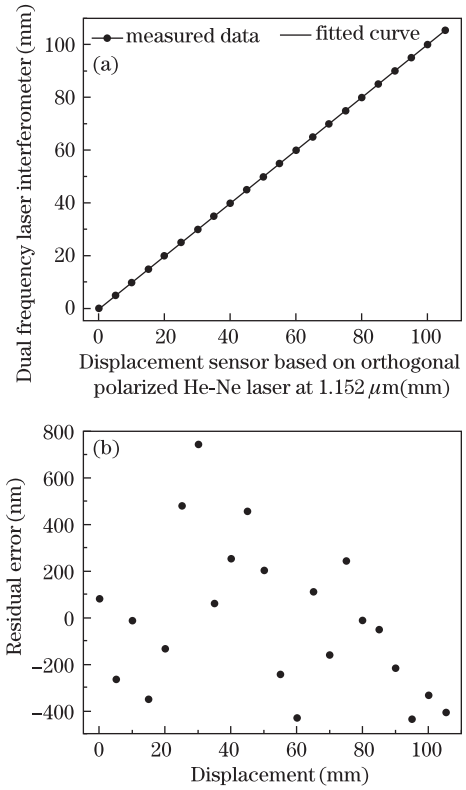

Fig. 5. Comparing the experiments between the displacement sensor and the interferometer: (a) comparison results and (b) residual error.

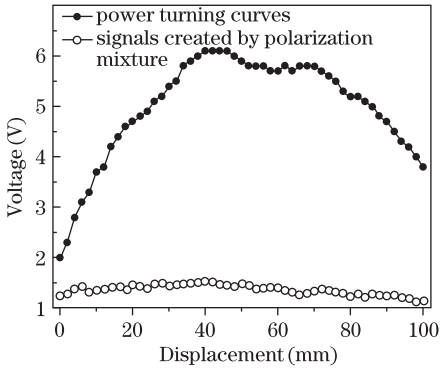

Fig. 6. Changes in the magnitude of the power tuning curves and the signals created by the polarization mixture.

laser interferometer shows that the linearity is 7×10^{-6} in the range of 100 mm with the resolution being 144 nm. Further experiments show that the displacement measuring stability based on the method of polarization mixture is better than that of the power tuning curves.

The authors are grateful to Matthias Dilger from Germany for the polishing work of this letter. This work was supported by the National Natural Science Foundation of China under Grant Nos. 60827006 and 60723004.

References

1. F. Brizuela, S. Carbajo, A. Sakdinawat, D. Alessi, D. H. Martz, Y. Wang, B. Luther, K. A. Goldberg, I. Mochi, D. T. Attwood, B. L. Fontaine, J. J. Rocca, and C. S. Menoni, Opt. Express **18,** 14467 (2010).
2. J. A. M. Rodriguez, Appl. Opt. **47,** 3590 (2008).
3. V. F. Gamalii, J. Appl. Spectrosc. **62,** 1001 (1995).
4. S. Gonchukov, M. Vakurov, and V. Yermachenko, Laser Phys. Lett. **3,** 314 (2006).
5. J. Wang, R. Zhu, J. Zhou, H. Zang, X. Zhu, and W. Chen, Chin. Opt. Lett. **9,** 081405 (2011).
6. J. A. M. Rodriguez, J. Mod. Opt. **57,** 1583 (2010).
7. J. A. M. Rodriguez and R. R. Vera, J. Mod. Opt. **52,** 1385 (2005).
8. W. Du, S. Zhang, and Y. Li, Opt. Laser Eng. **43,** 1214 (2005).
9. S. Zhang, *Principle of Orthogonal Polarized Lasers* (in Chinese) (Tsinghua University Press, Beijing, 2005).
10. Y. Han, Y. Zhang, L. Yan, and S. Zhang, Opt. Laser Eng. **31,** 207 (1999) .
11. Z. Hu, S. Zhang, W. Liu, and H. Jia, Opt. Laser Technol. **42,** 540 (2010).
12. Z. Zhao, S. Zhang, Y. Tan, and Y. Li, Chin. Opt. Lett. **10,** 021402 (2012).
13. Z. Xu, S. Zhang, W. Du, and Y. Li, Opt. Commun. **265,** 270 (2006).